MAHDI NEKOUEI*, KAVEH AHANGARI**

MODIFIED STABILITY CHARTS FOR ROCK SLOPES BASED ON THE HOEK-BROWN FAILURE CRITERION

ZMODYFIKOWANE DIAGRAMY STABILNOŚCI SKALISTYCH ZBOCZY OTRZYMANE W OPARCIU O WARUNEK WYTRZYMAŁOŚCI HOEKA-BROWNA

Only an article rendered by Lia et al. in 2008 has represented charts based on Hoek-Brown criterion for rock slopes, however, these charts are not precise and efficient. Because of this problem, a modification is suggested for the mentioned charts in this study. The new charts are calculated according to four methods. Among the methods, one relates to finite element method using *Phase2* software. The other three methods are Janbu, Bishop and Fellenius that belong to limit equilibrium method by using *Slide* software. For each slope angle, the method having high correlation coefficient is selected as the best one. Then, final charts are rendered according to the selected method and its specific equations. Among forty equations, twenty-five ones or 62.5% relate to numerical method and *Phase2* software, six ones or 15% belong to Fellenius limit equilibrium, six ones or 15% relate to Bishop limit equilibrium, and three ones or 7.5% belong to Janbu limit equilibrium. In order to validate new charts, slope stability analysis is carried out for several sections of Chadormalu iron ore open pit mine, Iran. The error percentage of new charts in limit equilibrium method using *Slide* software and in Bishop method for slopes of Chadormalu iron ore mine are rendered and compared. The charts on a basis of Hoek-Brown failure criterion for rock slopes show less than ±4% error. This indicates that these charts are appropriate tools and their safety factor is optimal for rock slopes.

Keywords: Stability charts; Rock slopes, Hoek-Brown criterion

Diagramy stabilności skalistych zboczy otrzymane w oparciu o warunek wytrzymałości Hoeka-Browna znaleźć można jedynie w pracy Lia et al. (2008), choć wykresy te nie są absolutnie dokładne i jasne. Dlatego też w niniejszym artykule zaproponowano pewną modyfikację diagramów. Nowe wykresu sporządzono w oparciu o cztery metody. Jedna z metod opiera się na metodzie elementów skończonych i wykorzystuje oprogramowanie *Phase2*. Pozostałe trzy podejścia to metody Janbu, Bishopa i Felleniusa,

---
* DEPARTMENT OF MINING ENGINEERING, SCIENCE AND RESEARCH BRANCH, ISLAMIC AZAD UNIVERSITY, TEHRAN, IRAN, E-MAIL: MAHDI.NEKOUEI@GMAIL.COM
** DEPARTMENT OF MINING ENGINEERING, SCIENCE AND RESEARCH BRANCH, ISLAMIC AZAD UNIVERSITY, TEHRAN, IRAN.
CORRESPONDING AUTHOR: E-mail: kaveh.ahangari@gmail.com

748

bazujące na metodzie równowagi granicznej i wykorzystujące oprogramowanie *Slide*. Dla każdego kąta nachylenia zbocza, wybierana jest metoda najskuteczniejsza, czyli taka która zapewnia wysoki współczynnik korelacji. Następnie sporządzane są wykresy końcowe, zgodnie w wybraną metodą i z wykorzystaniem odpowiednich równań. Spośród 40 równań, 25 z nich (czyli 62.5%) odnosi się do metod numerycznych (oprogramowanie *Phase2*), sześć równań (15%) należy do metody równowagi granicznej Felleniusa, kolejne sześć równań (15%) ma odniesienie do metody równowagi granicznej Bishopa, zaś trzy równania (7.5%) należą do metody równowagi granicznej Janbu. W celu walidacji nowych diagramów, przeprowadzono analizę stabilności zboczy na kilku wybranych odcinkach kopalni odkrywkowej rud żelaza w Chadormalu, Iran. Następnie porównano otrzymane procentowe wskaźniki niedokładności nowych diagramów uzyskanych za pomocą metody równowagi granicznej i przy wykorzystaniu oprogramowania *Slide* oraz w metodzie Bishopa obliczone dla zboczy kopalni rud żelaza Chadormalu. Diagramy uzyskane na podstawie warunku stabilności Hoeka-Browna dla zboczy w kopalni dają wskaźnik błędu na poziomie ±4%. Oznacza to, że diagramy takie są odpowiednimi narzędziami a współczynniki bezpieczeństwa dla zboczy skalnych wyliczone na ich podstawie uznać można za optymalne.

Słowa kluczowe: wykresy stabilności, zbocza skalne, warunek wytrzymałości Hoeka-Browna

1. Introduction

One of the main difficulties for mining and rock mechanic engineers is stability estimation of rock slopes. The estimation and stability control using failure is one of the most complicated matters.

There are various methods for recognizing rock slope stability. Some methods are the direct control of slope behavior during its life using the measurement methods (Marschalko et al., 2008). One of the common methods for primary estimation of rock slope stability and even performing rock slope stability is using their charts. In particular, in order to predict rock slope stability, experts use stability charts of soil, which were rendered by Taylor (1937). Moreover, researchers utilize Hoek and Bray (1981) and Zanbak (1983) charts, which are respectively based on Mohr-Coulomb failure criterion and for stability in toppling rock slopes. In order for designing the above-mentioned charts, failure criterion factors of intact rock such as internal friction angle and cohesion are necessary for input data. Calculating internal friction angle and cohesion for rock mass is difficult and generalizing them to bulk rock mass is not appropriate. Collins et al. (1988) and also Drescher and Christopoulos (1988) rendered tangential strength parameters (C_t and φ_t) for nonlinear failure criterion for estimating slope stability. One of the common methods for estimating the strength of rock mass is Hoek-Brown failure criterion (Hoek et al., 2002) because it explains the rock mass in a comprehensive way. Only the studies performed by Yang et al. (Yang et al., 2004a, 2004b, 2006) were on a basis of the latest interpretation of Hoek-Brown failure criterion. They obtained optimum based on Hoek-Brown failure criterion for rock slopes. Only an article rendered by Lia et al. (Lia et al., 2008) has represented charts based on Hoek-Brown criterion for rock slopes, however, these charts are not precise and efficient.

The rendered charts on a basis of Hoek-Brown failure criterion for rock slopes are modified in current study. Dried or completely drained slopes that have no tensile crack or have circular failure are used. In addition, assumed data based on engineering principles (it contains a wide range of weak to strong rocks) are utilized for modifying rock slope stability charts that are on a basis of Hoek-Brown failure criterion using limit equilibrium method with *Slide* limit equilibrium software (Rocscience, 2D limit equilibrium analysis software, Slide 5.0) and finite element method using *Phase2* software (Rocscience, PHASE2. 2D finite element software).

Finally, in order for confirming the accuracy of rendered charts, slope stability of various sections of Chadormalu mine, Iran, is carried out and these charts are compared with the charts that were drawn by SRK company (SRK and Kani Kavan Shargh 2006) using limit equilibrium analysis for this mine. The error percentage of these charts will be mentioned.

2. Researching method

Empirical Hoek-Brown failure criterion has been suggested for isotropic environment and is an appropriate factor for estimating the strength of rock mass. Where shear fractures are created by a preferential direction and/or are controlled by an assemblage of ruptures or a combination of several discontinuities, the isotropic assumption for Hoek-Brown failure criterion in slope stability is not appropriate. Therefore, Hoek et al. (2002) believes that Hoek-Brown failure criterion is applicable for intact rock and heavily jointed rock mass. Hoek-Brown failure criterion is not applicable for lopes with anisotropic rock properties. In current study, rock mass in all slopes is assumed as first group. Therefore, Hoek-Brown failure criterion is applicable for this type of slopes. Applicability and *GSI* system limitation are described by Hoek et al. (1998), Marinos et al. (2004a), Marinos et al. (2004b), Sonmez and Ulusay (1999), Cai et al. (2004) and Russo (2009). According to Hoek et al. (2002) theory, Hoek-Brown failure criterion is defined by following equations:

$$\sigma_1^/ = \sigma_3^/ + \sigma_{ci}(m_b \frac{\sigma_3^/}{\sigma_{ci}} + s)^\alpha \tag{1}$$

where,

$$m_b = m_i \exp(\frac{GSI - 100}{28 - 14D}) \tag{2}$$

$$s = \exp(\frac{GSI - 100}{9 - 3D}) \tag{3}$$

$$\alpha = \frac{1}{2} + \frac{1}{6}(e^{-GSI/15} - e^{-20/3}) \tag{4}$$

According to the above-mentioned equations, the values of a, s and m_b based on GSI Geologic Strength Index describe the quality of rock mass. In addition, *D* is degree of disturbance of the environment. Plane strain illustration from slope stability is shown in Fig. 1.

Jointed rock mass has intact uniaxial compressive strength (σ_{ci}), intact rock constant (m_i) and specific weight (γ). The value of specific weight is estimable from core samples. In order to estimate *GSI*, excavation is carried out in slopes. Slope geometry that defines height and slope angle of rock slope is respectively determined by *H* and *β*. Rock mass properties including intact uniaxial compressive strength, geologic strength index and intact rock constant parameters are respectively determined with σ_{ci}, *GSI* and m_i.
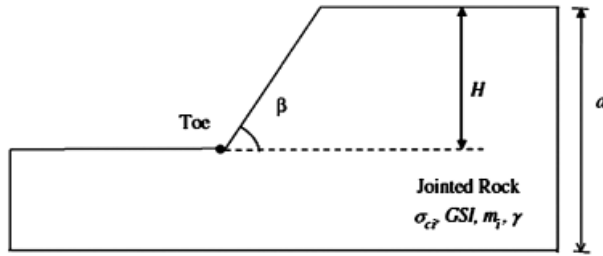
Fig. 1. Plane strain resulting from slope stability and the properties of slope and used parameters

The suggested parameters must have all parameters of Hoek-Brown failure criterion. In addition, they must include wide range of rocks consisting of weak, moderate, and hard. *GSI*, m_i, σ_{ci}, and *D* are principle parameters of Hoek-Brown failure criterion.

The other important parameters are γ, *H*, and β, which are related to slope geometry and specific weight. The range of these three parameters must be determined. Therefore, variable parameters in this study are *GSI*, m_i, σ_{ci}, γ, *H*, *D*, and β. The range of the mentioned parameters is given in Table 1 and also the reason of using them is explained.

TABLE 1

Ranges of *GSI*, m_i, σ_i, γ, and *H* parameters

H (m)	*GSI*	m_i	σ_{ci} (MPa)	γ (MN/m^3)	Slope Angle β	*D*
25	10	5	1	0.02	20	0.7
50	30	15	5	0.024	40	1
100	50	25	25	0.027	60	-
200	70	35	50	0.03	80	-
-	100	-	100	-	-	-

A range of 5-35 considered for m_i is according to guidance of *Roclab* software. The values less than 5 and over 35 do not belong to any type of rock in this software. This means that this range of m_i is considered for weak to hard rocks.

Intact uniaxial compressive strength (σ_{ci}) ranges from 1 to 100 MPa. This range is based on Hoek (2006), which indicates that it relates to weak to hard rocks.

The range of γ (specific weight) contains rocks that have 0.027 (MN/m^3). This uses for various rocks.

The ranges of disturbance factor, *D*, is from 0.7 to 1 and it is based on Hoek et al. (2002) suggestion. The ranges of *GSI*, *H* and β are selected according to engineering experiences.

Slope stability analysis is carried out by limit equilibrium method using *Slide* software and based on Bishop, Fellenius, Janbu (Rocscience, 2D limit equilibrium analysis software, Slide 5.0), and finite element methods using *Phase2* software (Rocscience, PHASE2. 2D finite element software) .

Slope stability charts of this study are drawn according to Hoek-Brown failure criterion for rock slopes in two methods of limit equilibrium and numerical. The limit equilibrium method is performed by 2D *Slide* software. Using vertical shear techniques, *Slide* software analyzes circular

and non-circular surfaces in rock and soil. Limit equilibrium methods are generally divided into three groups. 1 – Methods provide force equilibrium. 2 – Methods provide moment equilibrium. 3 – Methods provide both force and moment equilibriums. Bishop, Fellenius, and Janbu methods (Rocscience, 2D limit equilibrium analysis software, Slide 5.0) are used in this study. The main cause of selecting these three methods is that each of them provides one of the three groups of limit equilibrium method, that is, respectively, Janbu, Fellenius, and Bishop methods provide force, moment, and both force and moment equilibriums. *Slide* software is utilized in this study. The software uses slope search method for finding a surface with the least value of safety factor in screen (Rocscience, 2D limit equilibrium analysis software, Slide 5.0).

Furthermore, slope stability charts based on Hoek-Brown failure criterion for rock slopes are calculated by using finite element method and *Phase2* software. This software has been rendered by Rocscience Company and has been used for stability analysis in underground and open pit mines. The software is capable for 2D stress analysis around drilling and slope sections. In order to calculate safety factor of slopes, shear strength reduction method is used in current paper. In this method, a surface having the least shear strength reduction is considered as critical surface and obtained number is assumed as critical shear strength reduction factor or the least safety factor in a part of slope that has the least shear strength (Rocscience, PHASE2. 2D finite element software).

3. Slope stability charts based on Hoek-Brown failure criterion for rock slopes

By using *Slide* and *Phase2* software, the value of safety factor is calculated with four methods. As Table 1 shows, for each slope angle, 3200 models are created in both of the software. Totally, 12800 models are created by *Slide* software and 12800 models are built by *Phase2* software. In addition, 51200 values of safety factors are obtained from the four mentioned methods. Finally, for each slope angle, a method, which has the highest correlation coefficient among the methods, is selected as the best one and the final chart is rendered according to it and its relevant equation.

In all charts rendered in this paper, all horizontal or *x*-axes are based on $(0.0034 \times \sigma_{ci} \times m_i^{0.8}) / (\gamma \times H)$ (dimensionless) and all vertical or y-axes are based on $(0.0034 \times \sigma_{ci} \times m_i^{0.8} \times SF) / (\gamma \times H)$ (dimensionless). Both *x*- and *y*-axes are logarithmic. The present curves in each chart relate to various values of *GSI*.

Figs 2-4, and 5 are based on 20 degrees slope angle and 0.7 disturbance factor and are respectively relate to Fellenius, Bishop, Janbu, and *Phase2* methods. On the other hand, Fig. 6-9 are according to 20 degrees slope angle and 1 disturbance factor and are respectively belong to Fellenius, Bishop, Janbu, and *Phase2* methods.

Appendix 1 represents the charts related to Fellenius, Bishop, Janbu, and *Phase2* according to 40, 60, and 80 degrees slope angles with 0.7 and 1 disturbance factors.

Table 2 indicates disturbance factor, equation, and correlation coefficient related to *GSI*, and each method for each slope angle.

The yellow parts of this table show equations that have the highest values of correlation coefficient among the methods that are separated by disturbance factor related to *GSI* and each method for each slope angle.
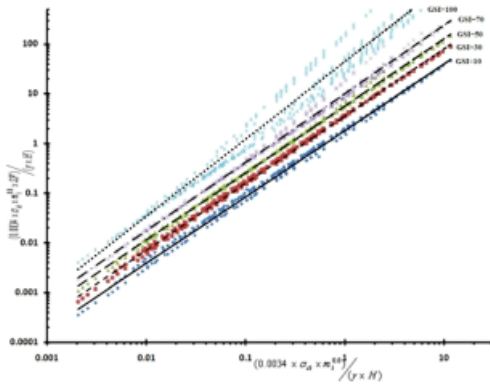
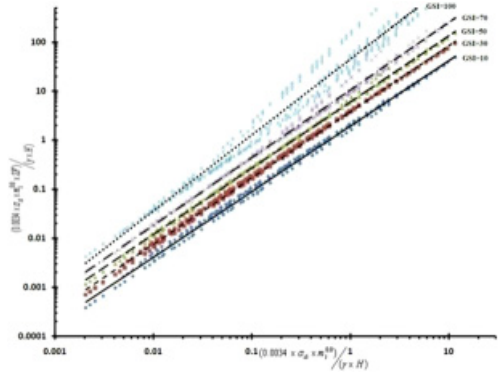Fig. 2. 20 degrees slope angle and 0.7 disturbance factor using Fellenius method

Fig. 3. 20 degrees slope angle and 0.7 disturbance factor using Bishop method
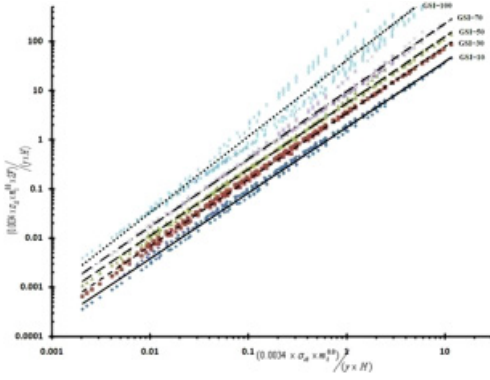

Fig. 4. 20 degrees slope angle and 0.7 disturbance factor using Janbu method
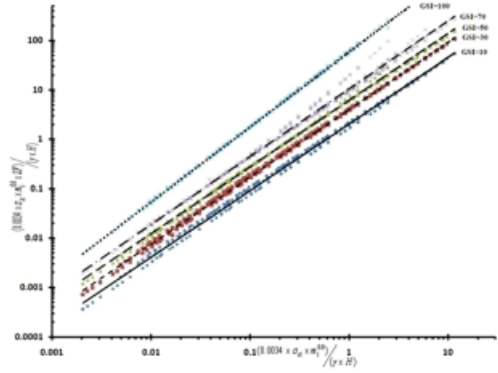

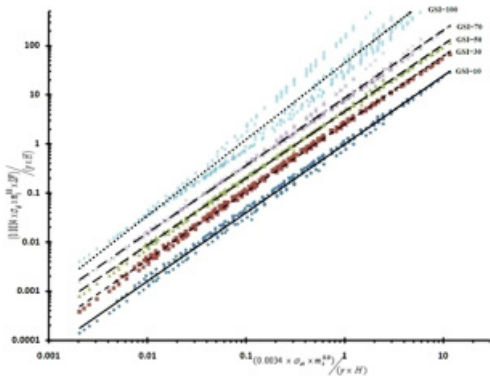Fig. 5. 20 degrees slope angle and 0.7 disturbance factor using Phase2 method

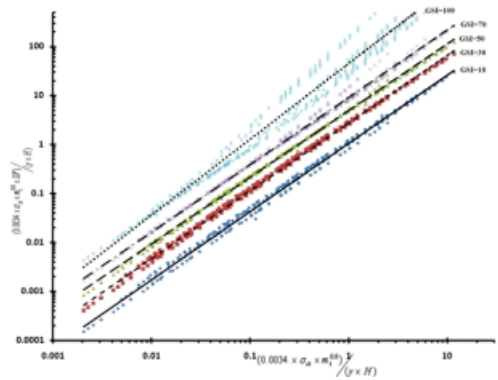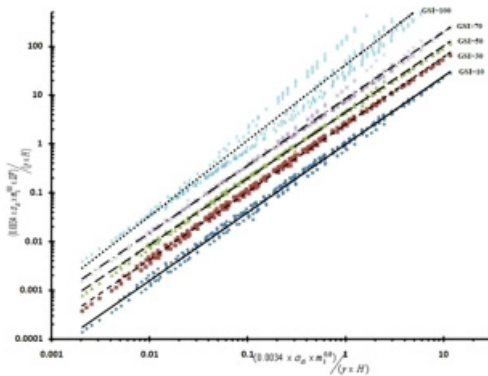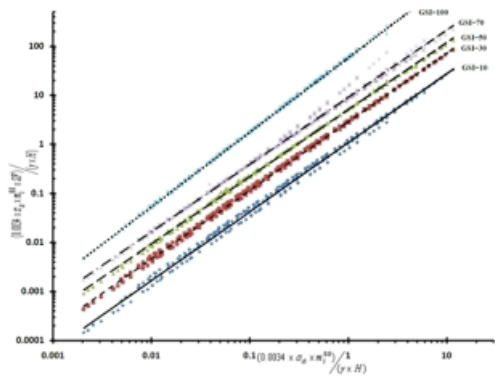Fig. 6. 20 degrees slope angle and 1 disturbance factor using Fellenius method

Fig. 7. 20 degrees slope angle and 1 disturbance factor using Bishop method

Fig. 8. 20 degrees slope angle and 1 disturbance
factor using Janbu method

Fig. 9. 20 degrees slope angle and 1 disturbance
factor using Phase2 method

Fig. 10 belongs to 20 degrees slope angle and 0.7 disturbance factor and is based on the equations rendered in Table 2 that have the highest correlation coefficient and are marked in yellow color. Moreover, Fig. 11 relates to 20 degrees slope angle and 1 disturbance factor and is based on the equations given in Table 2 that have the highest values of correlation coefficient. These values are also determined in yellow color.

Fig. 12 relates to 40 degrees slope angle and 0.7 disturbance factor. The Figure is according to the equations of Table 2 that has the highest values of correlation coefficient. These values are marked in yellow color. Fig. 13 relates to 40 degrees slope angle and 1 disturbance factor. It is based on the equations represented in Table 2 that has the highest values of correlation coefficient. These values are also determined in yellow color.

Fig. 14 relates to 60 degrees slope angle and 0.7 disturbance factor. This Figure is based on the equations rendered in Table 2 that has the highest values of correlation coefficient. The values are distinguished in yellow color. Furthermore, Fig. 15 belongs to 60 degrees slope angle and 1 disturbance factor. The Figure is also based on the equations of Table 2 that has the highest values of correlation coefficient and the values are determined with yellow color.

Fig. 16 relates to 80 degrees slope angle and 0.7 disturbance factor. This Figure is based on the equations given in Table 2 that has the highest correlation coefficient values and are determined with yellow color. Fig. 17 belongs to 80 degrees slope angle and 1 disturbance factor. It is based on Table 2 that has the highest values of correlation coefficient. The values are recognizable with yellow color.

Figs 10 to 17 relate to the best equations of Table 2. The equations are based on disturbance factor and slope angle. Forty equations are selected as the best one and the highest correlation coefficient values in Table 2. Among these equations, twenty-five ones (62.5%) relate to numerical method and *Phase2* software while six ones (15%) belong to Fellenius limit method. In addition, six equations (15%) relate to Bishop limit method and three ones (7.5%) belong to Janbu limit method. In slope angles, which are less than 60 degrees, the number of equations related to numerical method and have the highest correlation coefficient is more than the ones belonged to limit equilibrium methods. However, in slope angles, which are more than 60 degrees, this matter is versa and a number of equations that have the highest correlation coefficient and relate

TABLE 2

Equation and correlation coefficient related to each *GSI* and method for every slope angle

Slope angle	Methods (Disturbance Factor)	D = 0.7				D = 1			
		Fellenius	Bishop	Jambu	Phase 2	Fellenius	Bishop	Jambu	Phase 2
20	GSI = 10	$y = 1.810x^{1.336}$ $R^2 = 0.996$	$y = 1.932x^{1.335}$ $R^2 = 0.996$	$y = 1.791x^{1.337}$ $R^2 = 0.995$	$y = 2.024x^{1.348}$ $R^2 = 0.997$	$y = 0.979x^{1.394}$ $R^2 = 0.995$	$y = 1.045x^{1.393}$ $R^2 = 0.995$	$y = 0.968x^{1.395}$ $R^2 = 0.996$	$y = 1.075x^{1.407}$ $R^2 = 0.994$
	GSI = 30	$y = 3.540x^{1.351}$ $R^2 = 0.998$	$y = 3.788x^{1.350}$ $R^2 = 0.997$	$y = 3.482x^{1.350}$ $R^2 = 0.998$	$y = 3.989x^{1.363}$ $R^2 = 0.999$	$y = 2.548x^{1.384}$ $R^2 = 0.998$	$y = 2.727x^{1.383}$ $R^2 = 0.998$	$y = 2.507x^{1.383}$ $R^2 = 0.998$	$y = 2.900x^{1.399}$ $R^2 = 0.999$
	GSI = 50	$y = 5.661x^{1.350}$ $R^2 = 0.997$	$y = 6.049x^{1.349}$ $R^2 = 0.998$	$y = 5.540x^{1.348}$ $R^2 = 0.998$	$y = 6.208x^{1.351}$ $R^2 = 0.999$	$y = 4.560x^{1.360}$ $R^2 = 0.998$	$y = 4.873x^{1.360}$ $R^2 = 0.997$	$y = 4.464x^{1.359}$ $R^2 = 0.998$	$y = 5.109x^{1.369}$ $R^2 = 0.999$
	GSI = 70	$y = 9.911x^{1.379}$ $R^2 = 0.994$	$y = 10.55x^{1.379}$ $R^2 = 0.994$	$y = 9.618x^{1.376}$ $R^2 = 0.993$	$y = 10.58x^{1.374}$ $R^2 = 0.995$	$y = 8.580x^{1.375}$ $R^2 = 0.994$	$y = 9.070x^{1.373}$ $R^2 = 0.995$	$y = 8.327x^{1.372}$ $R^2 = 0.995$	$y = 9.138x^{1.369}$ $R^2 = 0.996$
	GSI = 100	$y = 44.07x^{1.556}$ $R^2 = 0.974$	$y = 45.16x^{1.548}$ $R^2 = 0.975$	$y = 41.85x^{1.550}$ $R^2 = 0.974$	$y = 58.82x^{1.520}$ $R^2 = 0.999$	$y = 44.07x^{1.556}$ $R^2 = 0.974$	$y = 45.16x^{1.548}$ $R^2 = 0.975$	$y = 41.85x^{1.550}$ $R^2 = 0.974$	$= 58.82x^{1.520}$ $R^2 = 0.999$
40	GSI = 10	$y = 1.020x^{1.328}$ $R^2 = 0.995$	$y = 1.091x^{1.326}$ $R^2 = 0.995$	$y = 1.012x^{1.328}$ $R^2 = 0.996$	$y = 1.132x^{1.336}$ $R^2 = 0.997$	$y = 0.570x^{1.385}$ $R^2 = 0.995$	$y = 0.609x^{1.382}$ $R^2 = 0.995$	$y = 0.565x^{1.385}$ $R^2 = 0.996$	$y = 0.631x^{1.395}$ $R^2 = 0.997$
	GSI = 30	$y = 2.050x^{1.346}$ $R^2 = 0.998$	$y = 2.187x^{1.342}$ $R^2 = 0.998$	$y = 2.027x^{1.345}$ $R^2 = 0.997$	$y = 2.247x^{1.345}$ $R^2 = 0.999$	$y = 1.483x^{1.373}$ $R^2 = 0.998$	$y = 1.582x^{1.369}$ $R^2 = 0.998$	$y = 1.467x^{1.373}$ $R^2 = 0.998$	$y = 1.669x^{1.379}$ $R^2 = 0.999$
	GSI = 50	$y = 3.418x^{1.358}$ $R^2 = 0.997$	$y = 3.619x^{1.353}$ $R^2 = 0.997$	$y = 3.372x^{1.356}$ $R^2 = 0.997$	$y = 3.588x^{1.341}$ $R^2 = 0.998$	$y = 2.715x^{1.362}$ $R^2 = 0.997$	$y = 2.875x^{1.357}$ $R^2 = 0.998$	$y = 2.678x^{1.361}$ $R^2 = 0.997$	$y = 2.916x^{1.352}$ $R^2 = 0.999$
	GSI = 70	$y = 6.535x^{1.410}$ $R^2 = 0.991$	$y = 6.805x^{1.402}$ $R^2 = 0.992$	$y = 6.442x^{1.411}$ $R^2 = 0.990$	$y = 6.804x^{1.395}$ $R^2 = 0.991$	$y = 5.579x^{1.403}$ $R^2 = 0.993$	$y = 5.810x^{1.395}$ $R^2 = 0.991$	$y = 5.500x^{1.403}$ $R^2 = 0.992$	$y = 5.767x^{1.384}$ $R^2 = 0.992$
	GSI = 100	$y = 32.60x^{1.600}$ $R^2 = 0.956$	$y = 32.24x^{1.587}$ $R^2 = 0.969$	$y = 31.46x^{1.589}$ $R^2 = 0.964$	$y = 36.41x^{1.539}$ $R^2 = 0.997$	$y = 32.60x^{1.600}$ $R^2 = 0.956$	$y = 32.24x^{1.587}$ $R^2 = 0.969$	$y = 31.46x^{1.589}$ $R^2 = 0.964$	$y = 36.41x^{1.539}$ $R^2 = 0.997$

TABLE 2. continued

Equation and correlation coefficient related to each GSI and method for every slope angle

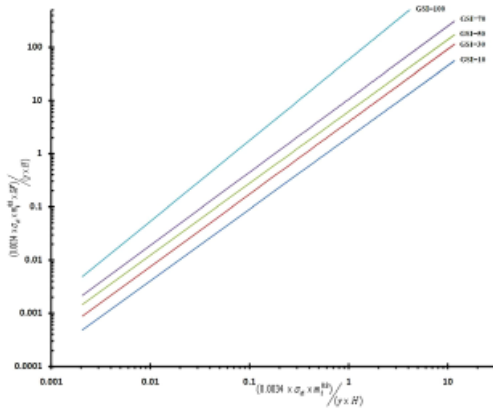| Disturbance Factor		D = 0.7				D = 1			
Slope angle	Methods / GSI	Fellenius	Bishop	Janbu	Phase 2	Fellenius	Bishop	Janbu	Phase 2
60	GSI = 10	$y = 0.659x^{1.319}$, $R^2 = 0.996$	$y = 0.696x^{1.315}$, $R^2 = 0.997$	$y = 0.657x^{1.320}$, $R^2 = 0.997$	$y = 0.708x^{1.326}$, $R^2 = 0.998$	$y = 0.38x^{1.372}$, $R^2 = 0.993$	$y = 0.401x^{1.367}$, $R^2 = 0.995$	$y = 0.378x^{1.373}$, $R^2 = 0.995$	$y = 0.430x^{1.401}$, $R^2 = 0.997$
	GSI = 30	$y = 1.368x^{1.343}$, $R^2 = 0.998$	$y = 1.427x^{1.335}$, $R^2 = 0.998$	$y = 1.354x^{1.341}$, $R^2 = 0.997$	$y = 1.395x^{1.324}$, $R^2 = 0.999$	$y = 0.990x^{1.364}$, $R^2 = 0.998$	$y = 1.033x^{1.356}$, $R^2 = 0.998$	$y = 0.980x^{1.362}$, $R^2 = 0.998$	$y = 1.052x^{1.356}$, $R^2 = 0.999$
	GSI = 50	$y = 2.395x^{1.367}$, $R^2 = 0.997$	$y = 2.452x^{1.358}$, $R^2 = 0.996$	$y = 2.362x^{1.366}$, $R^2 = 0.997$	$y = 2.349x^{1.336}$, $R^2 = 0.998$	$y = 1.886x^{1.366}$, $R^2 = 0.998$	$y = 1.931x^{1.356}$, $R^2 = 0.997$	$y = 1.860x^{1.364}$, $R^2 = 0.998$	$y = 1.826x^{1.330}$, $R^2 = 0.999$
	GSI = 70	$y = 4.869x^{1.434}$, $R^2 = 0.988$	$y = 4.895x^{1.422}$, $R^2 = 0.989$	$y = 4.919x^{1.439}$, $R^2 = 0.984$	$y = 4.988x^{1.418}$, $R^2 = 0.987$	$y = 4.118x^{1.423}$, $R^2 = 0.990$	$y = 4.141x^{1.412}$, $R^2 = 0.991$	$y = 4.160x^{1.428}$, $R^2 = 0.986$	$y = 4.165x^{1.404}$, $R^2 = 0.989$
	GSI = 100	$y = 25.48x^{1.622}$, $R^2 = 0.966$	$y = 25.43x^{1.616}$, $R^2 = 0.966$	$y = 30.69x^{1.642}$, $R^2 = 0.940$	$y = 25.37x^{1.558}$, $R^2 = 0.994$	$y = 25.48x^{1.622}$, $R^2 = 0.966$	$y = 25.43x^{1.616}$, $R^2 = 0.966$	$y = 30.69x^{1.642}$, $R^2 = 0.940$	$y = 25.37x^{1.558}$, $R^2 = 0.994$
80	GSI = 10	$y = 0.385x^{1.322}$, $R^2 = 0.999$	$y = 0.412x^{1.295}$, $R^2 = 0.998$	$y = 0.383x^{1.314}$, $R^2 = 0.998$	$= 0.240x^{1.318}$, $R^2 = 0.901$	$y = 0.234x^{1.367}$, $R^2 = 0.995$	$y = 0.251x^{1.339}$, $R^2 = 0.997$	$y = 0.233x^{1.359}$, $R^2 = 0.995$	$y = 0.141x^{1.3171}$, $R^2 = 0.901$
	GSI = 30	$y = 0.855x^{1.347}$, $R^2 = 0.994$	$y = 0.863x^{1.322}$, $R^2 = 0.995$	$y = 0.843x^{1.340}$, $R^2 = 0.999$	$y = 0.781x^{1.407}$, $R^2 = 0.968$	$y = 0.621x^{1.354}$, $R^2 = 0.996$	$y = 0.863x^{1.322}$, $R^2 = 0.995$	$y = 0.612x^{1.348}$, $R^2 = 0.999$	$y = 0.564x^{1.420}$, $R^2 = 0.967$
	GSI = 50	$y = 1.582x^{1.383}$, $R^2 = 0.995$	$y = 1.558x^{1.362}$, $R^2 = 0.996$	$= 1.567x^{1.382}$, $R^2 = 0.995$	$y = 1.585x^{1.460}$, $R^2 = 0.977$	$y = 1.230x^{1.372}$, $R^2 = 0.997$	$= 1.558x^{1.362}$, $R^2 = 0.996$	$y = 1.218x^{1.372}$, $R^2 = 0.996$	$y = 1.230x^{1.453}$, $R^2 = 0.977$
	GSI = 70	$y = 3.422x^{1.458}$, $R^2 = 0.986$	$y = 3.307x^{1.442}$, $R^2 = 0.987$	$y = 3.628x^{1.476}$, $R^2 = 0.975$	$y = 3.043x^{1.492}$, $R^2 = 0.938$	$y = 2.874x^{1.445}$, $R^2 = 0.988$	$y = 3.307x^{1.442}$, $R^2 = 0.987$	$y = 3.047x^{1.463}$, $R^2 = 0.978$	$y = 2.556x^{11.438}$, $R^2 = 0.939$
	GSI = 100	$y = 18.94x^{1.64}$, $R^2 = 0.965$	$y = 18.35x^{1.636}$, $R^2 = 0.964$	$y = 25.46x^{1.691}$, $R^2 = 0.931$	$y = 17.35x^{1.729}$, $R^2 = 0.944$	$y = 18.94x^{1.64}$, $R^2 = 0.965$	$y = 18.35x^{1.636}$, $R^2 = 0.964$	$y = 25.46x^{1.691}$, $R^2 = 0.931$	$y = 17.35x^{1.729}$, $R^2 = 0.944$

756

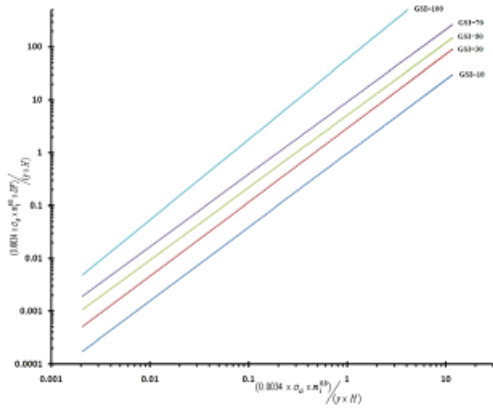Fig. 10. The best equations of Table 2 for 20 degrees slope angle and 0.7 disturbance factor

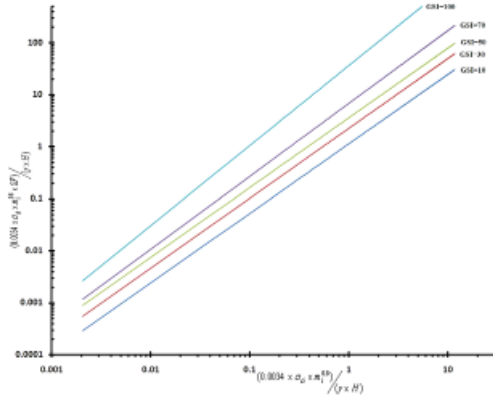Fig. 11. The best equations of Table 2 for 20 degrees slope angle and 1 disturbance factor

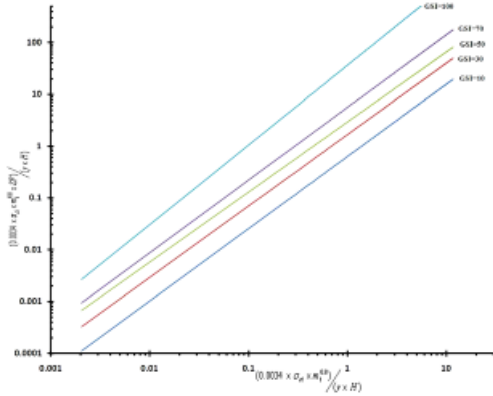Fig. 12. The best equations of Table 2 for 40 degrees slope angle and 0.7 disturbance factor

Fig. 13. The best equations of Table 2 for 40 degrees slope angle and 1 disturbance factor
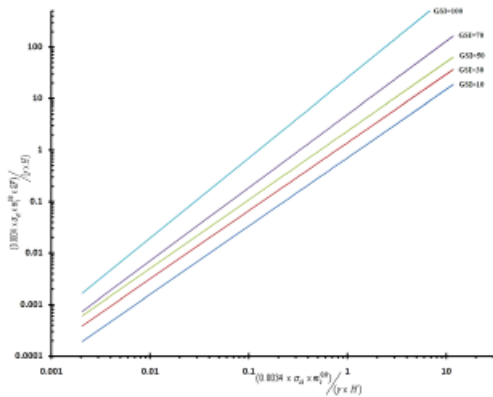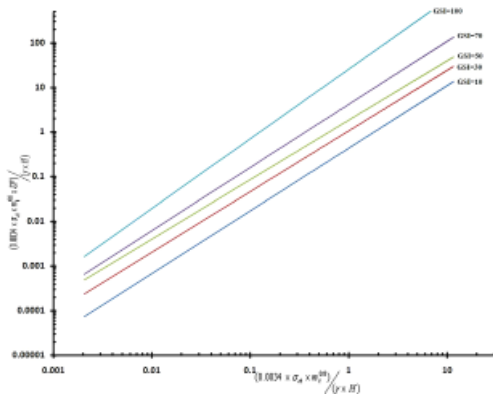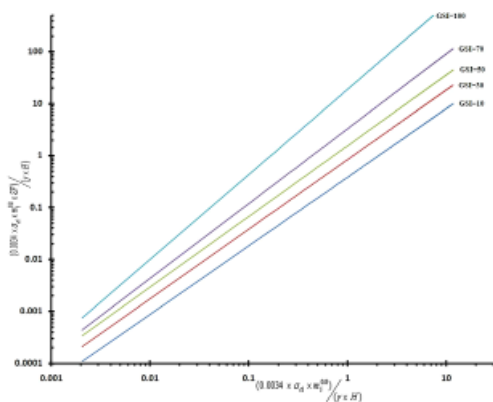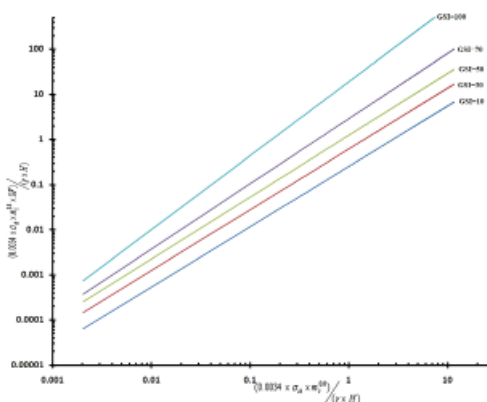

Fig. 14. The best equations of Table 2 for 60 degrees slope angle and 0.7 disturbance factor

Fig. 15. The best equations of Table 2 for 60 degrees slope angle and 1 disturbance factor

Fig. 16. The best equations of Table 2 for 80 degrees slope angle and 0.7 disturbance factor

Fig. 17. The best equations of Table 2 for 80 degrees slope angle and 1 disturbance factor

to limit methods is more than the ones belong to numerical methods. In order to use the charts, at first, rock slope angle and disturbance factor are determined, then, by considering the values of m_i, σ_{ci}, γ, and H, the amount of horizontal axis is obtained. By intersecting this amount with *GSI* curve and moving toward vertical axis, the value of safety factor, SF, is gained. It should be considered that vertical and horizontal axes are logarithmic.

4. Evaluation of the rendered charts in slopes of Chadormalu iron ore mine, Iran

The suggested charts are validated in several sections of the slopes of Chadormalu iron ore open pit mine in Iran. The mine is located in the center of Iran's Central Desert, northern flanks of gray-colored mountains of Chah Mohammad, southern margin of Saghand salt basin, 180 km northeast of Yazd city, 300 km south of Tabas city, and 65 km Choghart iron ore mine. The first pit of the mine is in form of a heart, which has respectively 960 m and 225 m width and depth. It has been designed for thirty years. In order to excavate Chadormalu mine using open pit method and its reconstruction as a pit, respectively, slope angle of pit, slope angle of wall face, width of safe bench, bench height, distance between safe benches, width of road, and ramp slope are considered 50-55°, 69.5°, 10 m, 15 m, 30 m, 25 m, and 8% (SRK and Kani Kavan Shargh 2006).

The first phase of stability studies in Chadormalu mine was carried out by SRK English Company and Kani Kavan Shargh Company in 2002. The main objective of these studies was preliminary recognition of the geologic structure of the mine, programming for collecting required information, and determining the areas that have failure potential. The information obtained from phase 2, designing for the slope of Chadormalu mine that was executed by SRK and Kani Kavan Shargh Companies, is used for validating the rendered charts in four sections of the mine.

Fig. 18 shows location and access roads of Chadormalu mine. Fig. 19 displays plan and zones of the mine. In order for validating the rendered charts, zones of southern 1, 2, 3, and 5 are utilized.
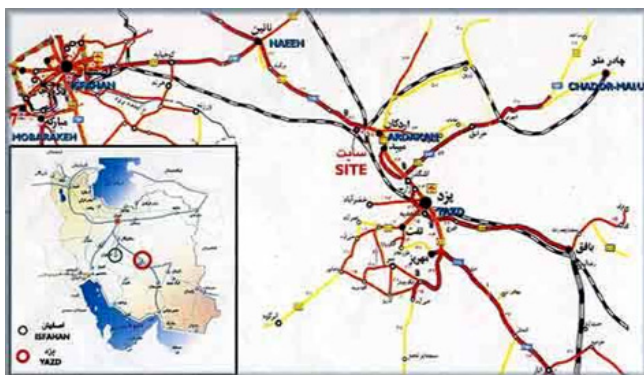
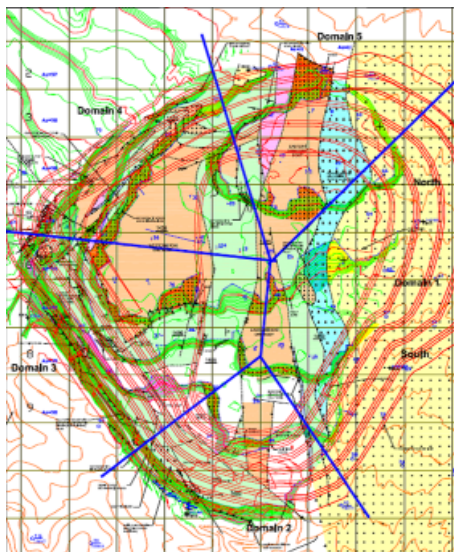Fig. 18. Location and access roads to Chadormalu mine

Fig. 19. Plan and zones of Chadormalu mine

TABLE 3

Values of required parameters for validating the rendered charts

H (m)	σ_{ci} (MPa)	GSI	Rock Slope Angle	m_i	γ (MN/m^3)	Borehole	D	Zone
150	59.089	27.92	40	22.71	0.0253	4	1	1- Southern
210	90.241	41.49	60	24.17	0.0275	5	1	3
135	70.713	35.50	60	25.19	0.0276	2	1	5
225	83.102	43.64	60	29.14	0.0319	3	1	2

The characteristics of the above-mentioned zones are given in Table 3. The required parameters for analysis are specific weight γ (MN/m^3), Hoek-Brown constant m_i, GSI, and intact uniaxial compressive strength σ_i (MPa). The parameters are obtained by the following equation in all parts of borehole. $\bar{a}$ is the average amount of parameter in all parts of borehole and a_i is the amount of parameter in l_i length.

$$\bar{a} = \frac{\sum a_i * l_i}{\sum l_i} \tag{5}$$

In slope stability analyses, which were carried out by SRK and Kani Kavan Shargh Companies, limit equilibrium program *SLOPE/W* and Bishop Method were used. Stability analysis for four sections of Chadormalu mine by using the rendered charts is executed in this study. The obtained results from charts are compared with the results of limit equilibrium program *SLOPE/W* and Bishop Method, carried out by SRK Company. Finally, the error percentage of the charts is determined. Respectively, Figs 20-23 represent stability analysis of zones of southern 1, 2, 3, and 5 by using limit equilibrium program *SLOPE/W*.
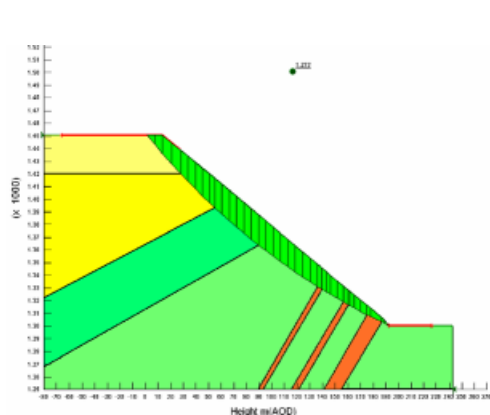
Fig. 20. Stability analysis of southern 1 zone using limit equilibrium program SLOPE/W
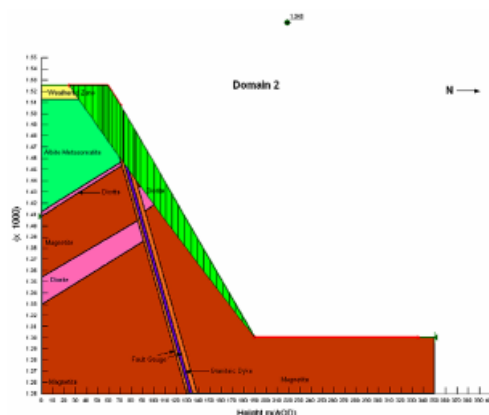
Fig. 21. Stability analysis of zone 2 using limit equilibrium program SLOPE/W

Table 4 indicates safety factor of slopes by using the rendered charts. Moreover, this table shows the information of Table 3. Furthermore, a comparison is carried out between the values of safety factor obtained from new charts and the results gained from limit equilibrium program *SLOPE/W*. The error percentage of the charts is recognized.

As Table 4 represents, the rendered charts based on Hoek-Brown failure criterion for rock slopes show the least error, less than ±4%, and are appropriate, quick, efficient, and trustable tool for calculating slope stability and safety factor.
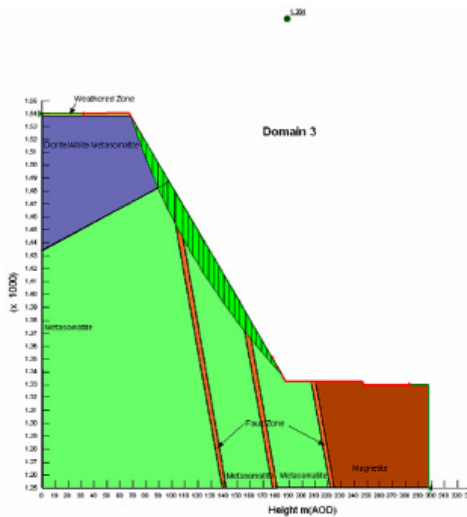
Fig. 22. Stability analysis of zone 3 using limit equilibrium program SLOPE/W
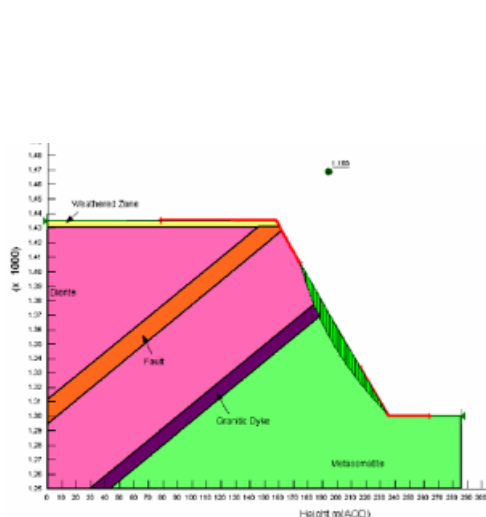
Fig. 23. Stability analysis of zone 5 using limit equilibrium program SLOPE/W

TABLE 4

Value of safety factor of slopes using the rendered charts and limit equilibrium program SLOPE/W

Error Percentage (%)	Value of safety factor of slope using limit equilibrium program SLOPE/W	Value of safety factor of slope using the rendered charts	Zone
3.382	1.277	1.318	1-Southern
3.917	1.264	1.313	3
3.121	1.161	1.196	5
1.833	1.343	1.318	2

5. Conclusion

The charts, which were rendered for rock slope stability, required the properties of intact rock as input parameters and these properties were generalized to rock mass. This matter caused to obtain high values of safety factor and led to gain slopes without any optimality and efficiency. Because of this matter, charts having rock mass properties as input parameters must be used. The charts rendered in this paper are based on Hoek-Brown failure criterion. The criterion represents complete properties of rock mass and causes to use them as input parameters for slopes. The charts are designed for slopes having no tensile crack or completely dried and drained slopes. These charts are based on two methods of slope stability analyses, which are limit equilibrium and finite element methods. *Slide* software, Bishop, Fellenius, and Janbu methods are used for limit equilibrium method whereas *Phase2* software is utilized for finite element method. According to Table 1, the charts are applicable for all types of rock masses. Among the above-mentioned

methods, by considering disturbance factor, slope angle, and *GSI*, the methods that have the highest correlation coefficient are selected as the best one and their equations are used as the best option. Final charts, based on disturbance factor and slope angle, according to Table 2 and yellow parts, are shown on a basis of the best equations. Figs 10 to 17 show the final charts. From having the highest correlation coefficient viewpoint, forty equations are selected as the best ones.

In order to evaluate and validate the rendered charts, slope stability analysis is carried out for several zones of the slopes of Chadormalu iron ore mine in Iran. The obtained results of the charts are compared with the stability analysis results of the designer of slopes in Chadormalu iron ore mine. It is concluded that the rendered charts on a basis of Hoek-Brown failure criterion for rock slope stability have the least error percentage, less than ±4%. This indicates that these charts are appropriate, quick, efficient, and trustable tool for calculating rock slope stability. Safety factors obtained from these charts are proper and optimal for slopes.

References

Cai M., Kaiser P.K., Uno H., Tasaka Y., Minami M., 2004. *Estimation of rock mass deformation modulus and strength of jointed hard rock masses using the GSI system*. Int. J. Rock Mech. Min. Sci., 41: 3-19.

Collins I.F., Gunn C.I.M., Pender M.J., Yan W., 1998. *Slope stability analyses for materials with a non-linear failure envelope*. Int. J. Numer Anal. Methods Geomech., 12: 533-50.

Drescher A., Christopoulos C., 1988. *Limit analysis slope stability with nonlinear yield conditions*. Int. J. Numer Anal. Methods Geome. 12 :341-345.

Hoek E., 2006.) *Practical Rock Engineering*. Rocscience, Vancouver.

Hoek E., Carranza-Torres C., Corkum B., 2002. *Hoek-Brown failure criterion-2002 edition*. In: Proceedings of the North American Rock Mechanics Symposium Toronto.

Hoek E., Marinos P., Benissi M., 1998. *Applicability of the geological strength index (GSI) classification for very weak and sheared rock masses*. The case of the Athens Schist Formation Bull. Eng. Geol. Env., 57: 153-155.

Hoek E., Bray J.W., 1981. *Rock slope engineering*. 3rd ed. Institute of Mining and Metallurgy, London.

Lia A.J., Merifielda A.V., Lyamin R.S., 2008. *Stability charts for rock slopes based on the Hoek–Brown failure criterion*. Int. J. Rock Mech. Min. Sci., 45: 689-700.

Marinos P., Hoek E., Marinos V., 2004a. *Variability of the engineering properties of rock masses quantified by the geological strength index*. *The case of ophiolites with special emphasis on tunneling*. In: Proceedings of the Rengers Symposium (Examples No. 5-8).

Marinos P., Marinos V., Hoek E., 2004b. *Geological strength index, GSI: applications, recommendations, limitations and alteration fields commensurately with the rock type*. In: Proceedings of the 10th International Congress. Bulletin of the Geological Society of Greece, vol. XXXVI, Thessaloniki.

Marschalko M., Fuka M., Třeslín L., 2008. *Measurements by the Method of Precise Inclinometry on Locality Affected by Mining Activity*. Arch. Min. Sci., Vol. 53, No. 3, p. 397-414.

Rocscience, 2D limit equilibrium analysis software. Slide 5.0. www.rocscience.com.

Rocscience, PHASE2. 2D finite element software. www.rocscience.com.

Russo G., 2009. *A new rational method for calculating GSI*. Tunneling and Underground Space Technology 24: 103-111.

Sonmez H., Ulusay R., 1999. *Modification to the geological strength index (GSI)*. Int. J. Rock Mech. Min. Sci., 36: 743-760.

SRK and Kani Kavan Shargh Consulting Engineers, 2006. *Report of phase 2 for designing slope stability of walls in Chadormalu Mine*.

Taylor D.W., 1937. *Stability of earth slopes*. J. Boston Soc. Civ. Eng., 24: 197-246.

Yang X.L., Zou J.F., 2006. *Stability factors for rock slopes subjected to pore water pressure based on the Hoek-Brown failure criterion*. Int. J. Rock Mech. Min. Sci., 43: 1146-52.

Yang X.L., Li L., Yin J.H., 2004a. *Stability analysis of rock slopes with a modified Hoek–Brown failure criterion*. Int. J. Numer Anal. Meth. Geomech 28: 181-90.

Yang X.L., Li L., Yin J.H., 2004b. *Seismic and static stability analysis for rock slopes by a kinematical approach*. Geotechnique 54(8): 543-9.

Zanbak C., 1983. *Design charts for rock slopes susceptible to toppling*. J. Geotech. Eng. Div. ASCE 190(8):1039-62.
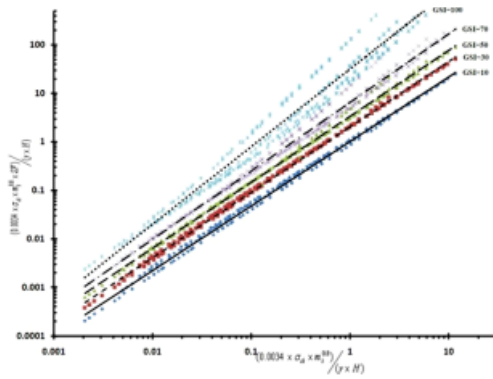
APPENDIX 1

Fig. 24. 40 degrees slope angle and 0.7 disturbance factor using Fellenius method
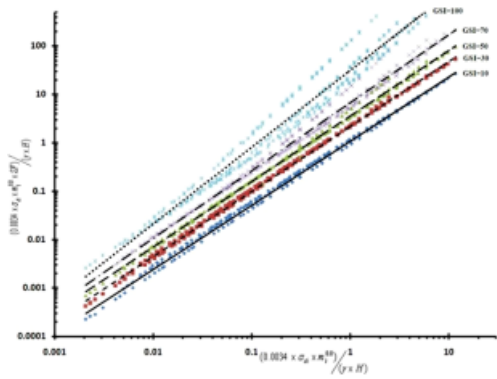
Fig. 25. 40 degrees slope angle and 0.7 disturbance factor using Bishop method
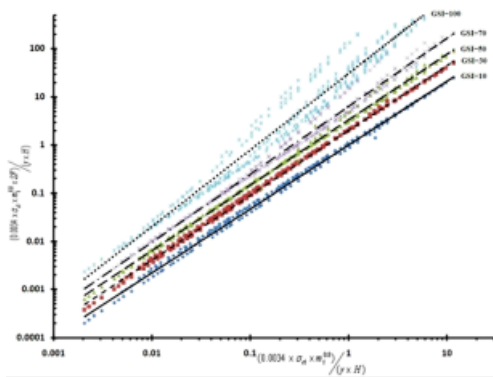
Fig. 26. 40 degrees slope angle and 0.7 disturbance factor using Janbu method
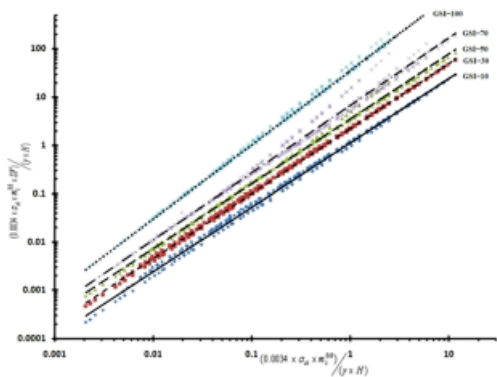
Fig. 27. 40 degrees slope angle and 0.7 disturbance factor using Phase2 method
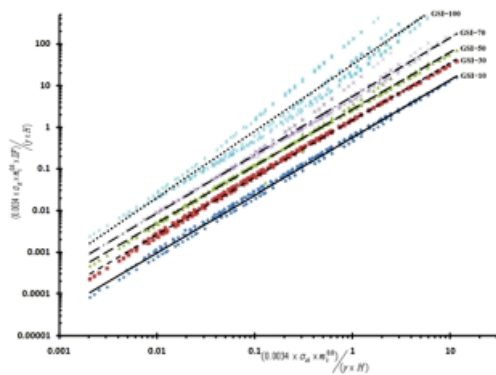
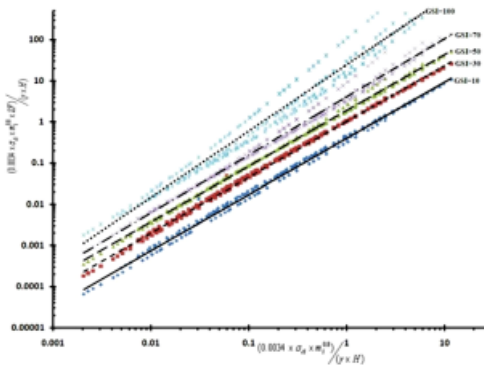Fig. 28. 40 degrees slope angle and 1 disturbance
factor using Fellenius method
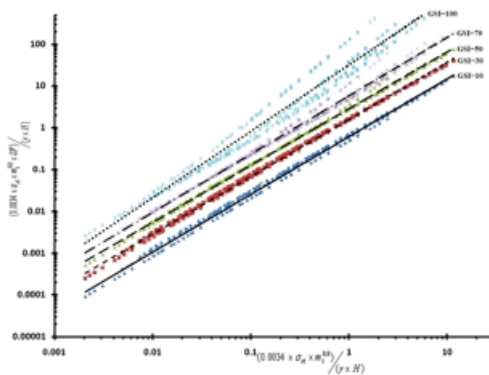
Fig. 29. 40 degrees slope angle and 1 disturbance
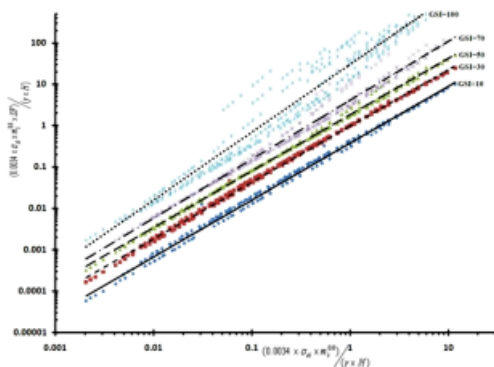factor using Bishop method
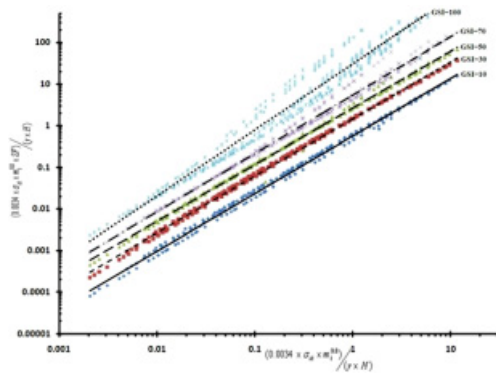
Fig. 30. 40 degrees slope angle and 1 disturbance
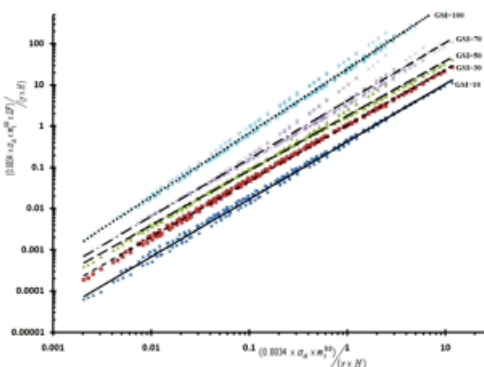factor using Janbu method
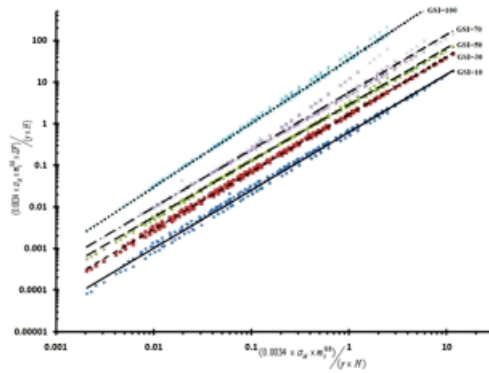
Fig. 31. 40 degrees slope angle and 1 disturbance
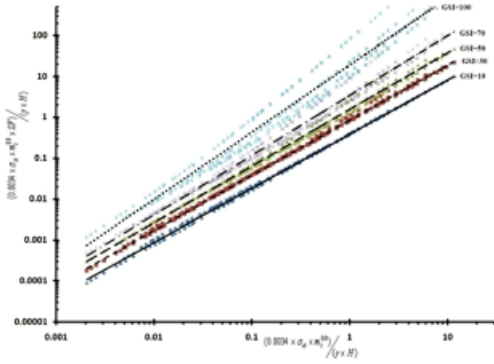factor using Phase2 method
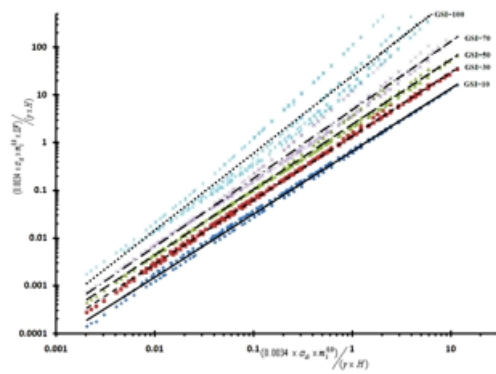
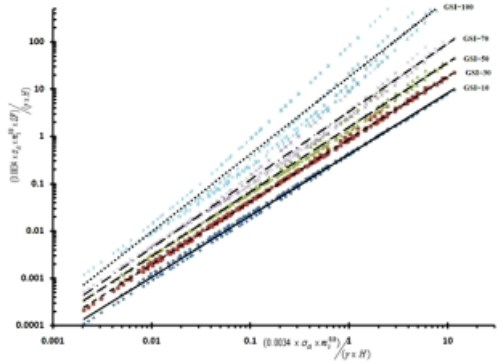Fig. 32. 60 degrees slope angle and 0.7 disturbance
factor using Fellenius method
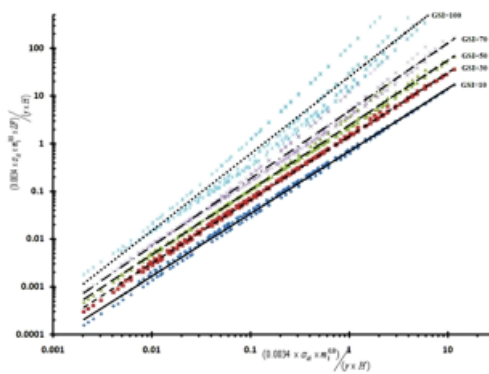
Fig. 33. 60 degrees slope angle and 0.7 disturbance
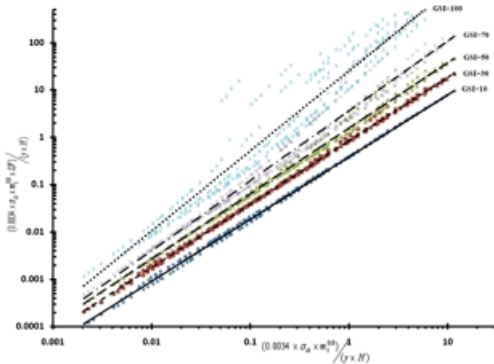factor using Bishop method
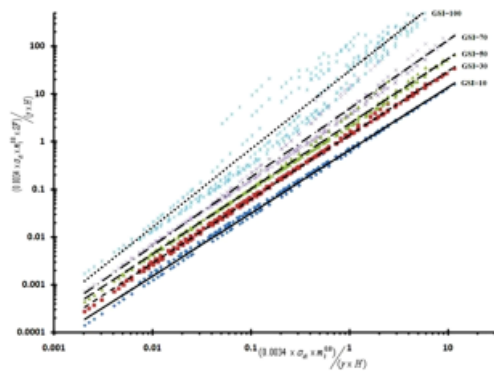
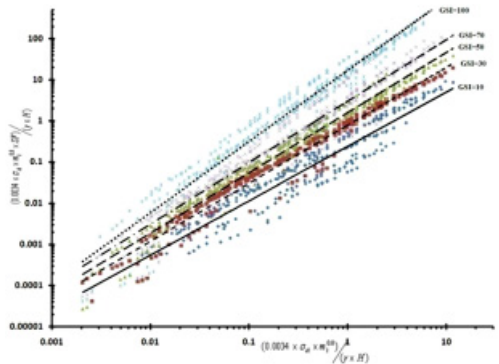Fig. 34. 60 degrees slope angle and 0.7 disturbance factor using Janbu method
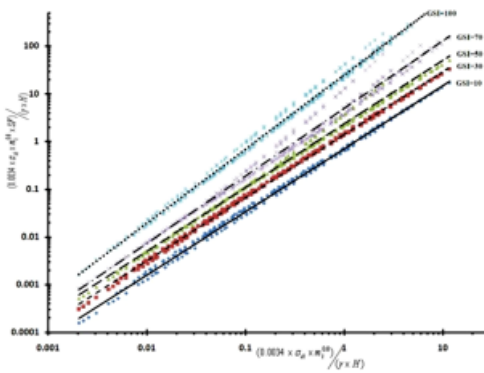
Fig. 35. 60 degrees slope angle and 0.7 disturbance factor using Phase2 method
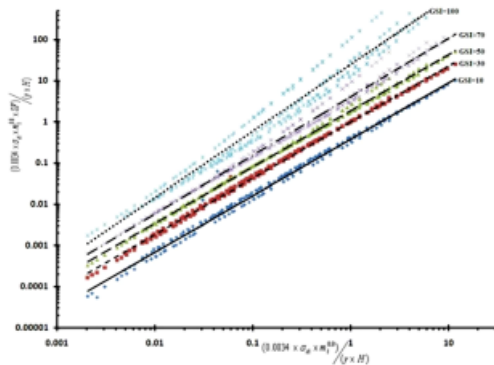
Fig. 36. 60 degrees slope angle and 1 disturbance factor using Fellenius method

Fig. 37. 60 degrees slope angle and 1 disturbance factor using Bishop method

Fig. 38. 60 degrees slope angle and 1 disturbance factor using Janbu method

Fig. 39. 60 degrees slope angle and 1 disturbance factor using Phase2 method

Fig. 40. 80 degrees slope angle and 0.7 disturbance
factor using Fellenius method

Fig. 41. 80 degrees slope angle and 0.7 disturbance
factor using Bishop method

Fig. 42. 80 degrees slope angle and 0.7 disturbance
factor using Janbu method

Fig. 43. 80 degrees slope angle and 0.7 disturbance
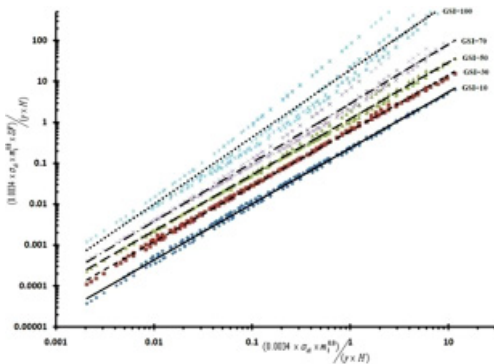factor using Phase2 method

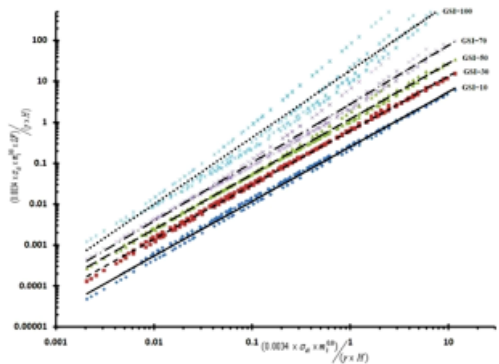Fig. 44. 80 degrees slope angle and 1 disturbance
factor using Fellenius method

Fig. 45. 80 degrees slope angle and 1 disturbance
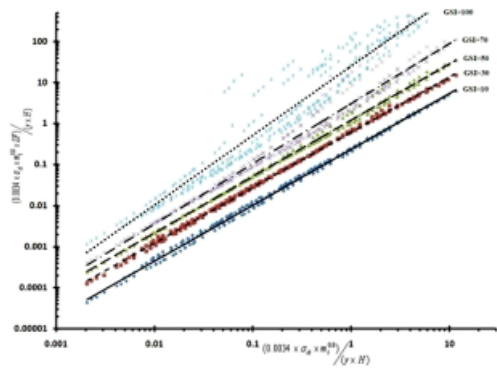factor using Bishop method

766

Fig. 46. 80 degrees slope angle and 1 disturbance
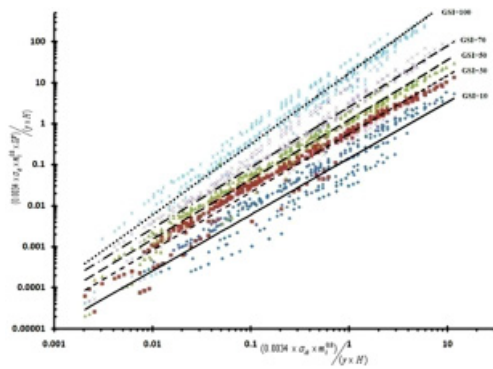factor using Janbu method

Fig. 47. 80 degrees slope angle and 1 disturbance
factor using Phase2 method